The Astronomical Journal, 133:284–289, 2007 January

METHANE AND ETHANE ON THE BRIGHT KUIPER BELT OBJECT 2005 FY9

M. E. Brown,[1] K. M. Barkume,[1] G. A. Blake,[1] E. L. Schaller,[1]
D. L. Rabinowitz,[2] H. G. Roe,[1] and C. A. Trujillo[3]
Received 2006 June 29; accepted 2006 September 26

ABSTRACT

The spectrum of the bright Kuiper Belt object 2005 FY9 from 0.34 to 2.5 μm is dominated by the red coloring of many outer solar system objects in the optical wavelength regime and by absorption due to methane in the near-infrared. The solid methane absorption lines are significantly broader on 2005 FY9 than on any other solar system body, indicating long optical path lengths through the methane. These long path lengths can be parameterized as a methane grain size of approximately 1 cm in a Hapke reflectance model. In addition to large-grained methane, the infrared spectrum also indicates the clear presence of ethane, an expected product of UV photolysis of methane. No evidence for N_2 or CO, both known to be present on Pluto, is found. We suggest that the large differences between the spectrum of 2005 FY9 and that of Pluto and 2003 UB313 is due to a depletion of nitrogen on the surface of 2005 FY9 that leads to large methane grains, abundant sites for ethane formation through UV photolysis, and highly irradiated tholin-like material.

Key words: comets: general — infrared: solar system — minor planets, asteroids

1. INTRODUCTION

While once Pluto appeared as a unique object in the far reaches of the solar system, the discovery of the Kuiper Belt caused the immediate realization that Pluto is a member of a much larger population. But while Pluto's orbit makes it a typical member of Kuiper Belt population dynamically, Pluto itself has still remained special as one of the few trans-Neptunian objects bright enough for detailed studies. Much of what we understand of the composition, density, and history of objects in the Kuiper Belt is put into context by studies of Pluto.

One of the primary motivations for our wide-field survey for distant objects in the solar system (Trujillo & Brown 2003) is to detect the largest members of the Kuiper Belt and to find a wider variety of objects bright enough to allow detailed physical study. The brightest object found in our survey to date is the scattered Kuiper Belt object 2005 FY9. Initial preliminary reports have already indicated that the surface of this object appears to resemble that of Pluto in that it is one of only four, after Pluto, Triton, 2003 UB313 (Brown et al. 2005), and Sedna (Barucci et al. 2005), to have clear detections of methane bands (Barkume et al. 2005; Licandro et al. 2006). Detailed study, of the types performed on Pluto, should reveal much about the composition, history, and interactions of the surface of this large Kuiper Belt object.

We have undertaken observations of the visible to near-infrared spectrum of 2005 FY9 using the Double Spectrograph at Palomar Observatory, the low- and medium-resolution infrared spectrometers at the Keck Observatory, and the 1.3 m SMARTS telescope. From these observations we discuss the state of the methane, additional surface components, and conclusions about the interactions of the surface and the atmosphere.

2. LOW-RESOLUTION SPECTROSCOPY

Low-resolution spectroscopy from 0.3 to 1.0 μm was obtained using the Double Spectrograph at the 5 m Hale Telescope (Oke & Gunn 1982) at Palomar Observatory, and spectroscopy from 1 to 2.5 μm was obtained using NIRC (Matthews & Soifer 1994), the facility near-infrared camera and spectrograph at the Keck Observatory. Visible photometry was obtained at the 1.3 m SMARTS telescope, while J and K_s photometry was obtained with NIRC. Most data were obtained on different dates, so significant light-curve variation could lead to relative errors between the photometric points. H. G. Roe et al. (2007, in preparation) have found that light-curve variations are below 0.04 mag and thus are unimportant for these results.

The visible spectra from Palomar were obtained on 2005 April 12 UT. The blue spectral channel covered 0.35–0.53 μm with a spectral resolution of $\sim$600, and the red spectra channel covered 0.63–1.0 μm microns with a resolution of $\sim$200. During observations the telescope tracked at the predicted rate of motion of 2005 FY9, and the spectral slit was oriented with the parallactic angle. The total integration time in both the blue and red channels was 900 s. The blue spectra were averaged over 10 pixels to increase the signal-to-noise ratio, lowering to a resolution of $\sim$80. A solar analog, Landolt 102-1081, was used for telluric calibration and to subtract the solar spectrum from 2005 FY9's reflectance spectrum. Wavelength calibration was performed using sky lines in the data.

The B, V, and I SMARTS visible photometry was obtained on 30 separate nights between 2005 April 4 and 2005 June 25. The observations and data reduction are described in Rabinowitz et al. (2007). The individual nights were averaged to obtain the results presented here.

The NIRC spectra were obtained on 2005 April 26 and 27. The data acquisition and reduction were identical to those described in Brown (2000). We obtained a total of 1600 s of integration in the HK setting, which covers from 1.4 to 2.5 μm, and 400 s of integration in the JH setting, which covers from 1.0 to 1.8 μm. Telluric calibration was performed by dividing the target spectrum by the spectrum of the nearby G2 V star HD 113338 obtained at a maximum difference of 0.1 air masses. NIRC photometry was obtained on the first night only, and the observations consisted of 60 s of integration in each of five nod positions in the J and K_s filter compared to infrared photometric standards observed at the same air mass.

The photometry and low-resolution spectra of 2005 FY9 are shown in Figure 1. The absolute value of the albedo is set from

[1] Division of Geological and Planetary Sciences, California Institute of Technology, Pasadena, CA, USA.
[2] Department of Physics, Yale University, New Haven, CT, USA.
[3] Gemini Observatory, Hilo, HI, USA.

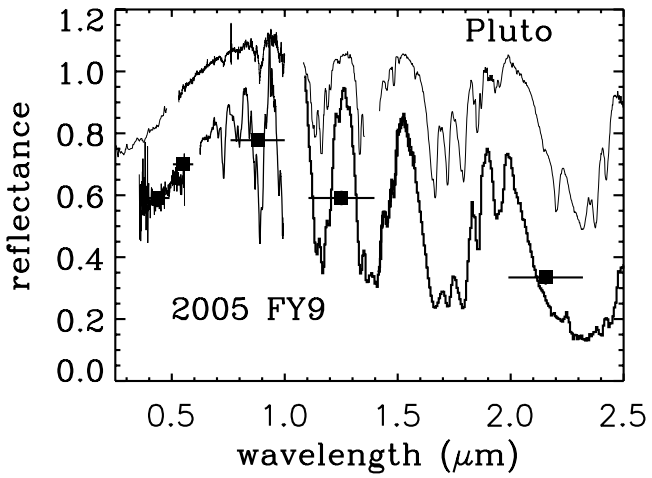

FIG. 1.—Absolute reflectance of 2005 FY9 (*lower line*) and of Pluto (*upper line*; shifted upward by 40%). The 2005 FY9 spectrum is a compilation of visible spectroscopy from Palomar Observatory, visible photometry from the SMARTS 1.3 m telescope, and infrared photometry and spectra from the Keck Observatory. The Pluto spectrum is a compilation from Trafton & Stern (1996), Grundy & Fink (1996), Rudy et al. (2003), and Douté et al. (1999). While the spectra of both objects are dominated by methane absorption, the methane lines of 2005 FY9 are significantly broader and more saturated. The spectral resolution of the data is approximately equal to 2 pixels on the detector, so the small-scale point-to-point variation in the spectrum is an accurate indication of the very small size of the errors in the spectrum.

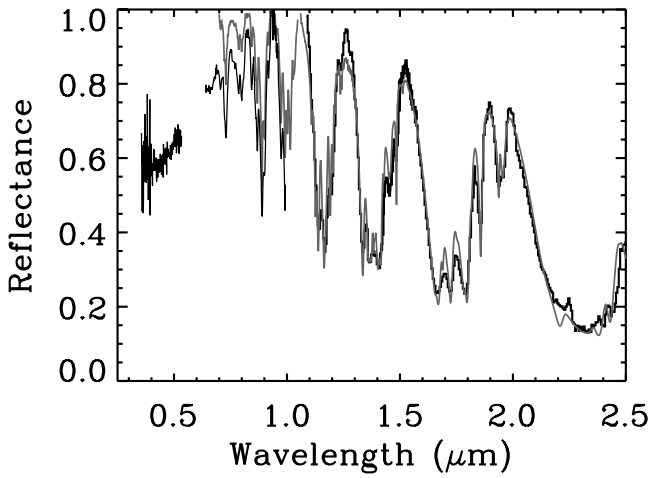

FIG. 2.—Reflectance of 2005 FY9 (*black line*) compared to a simple model (*gray line*) composed of 1 cm methane grains covering 80% of the surface and an infrared blue continuum covering 20%. The red optical spectrum requires that a red component be intimately mixed with the methane grains. The large methane grains provide an excellent fit to the infrared portion of the spectrum except beyond 2.2 μm, where additional absorbers are required.

Spitzer measurements of the size that imply a *V*-band albedo of 0.7 ± 0.1 (M. E. Brown et al. 2007, in preparation). Deep methane ice absorptions, initially reported by Barkume et al. (2005) and Licandro et al. (2006), dominate the red–to–near-infrared portion of the spectrum. Comparison with the spectrum of Pluto shows, however, that the methane absorptions features are significantly broader on 2005 FY9 than on Pluto. The breadth of these solid-state absorption features is a function of the typical optical path length traveled through the ice. The broad absorption features on 2005 FY9 suggest unusually long optical path lengths.

We model the spectrum using the approximations of Hapke (1993), where optical path length is parameterized as a grain size in a scattering regolith (see the Appendix for details on the spectral models). While the spectrum of Pluto can be modeled with methane grain sizes of $\sim$100 μm, the extreme breadth of the absorption of 2005 FY9 requires grain sizes of $\sim$1 cm. Such large path lengths cause the spectrum of methane ice to saturate at the centers of the strongest bands. The transmission through methane approaches zero at 1.7 μm and from 2.2 to 2.4 μm. The albedo of 2005 FY9 at these wavelengths is nonzero, however. Parts of the surface must therefore contain a component other than methane ice. At low resolution we simplistically model the nonmethane component as a spatially segregated uniformly colored continuum. A good fit to the near-infrared spectrum can be made with a Hapke model using strongly backscattering 1 cm methane grains covering 80% of the surface and a blue continuum with 100% reflectance at 1 μm and 50% reflectance at 2.5 μm covering the remaining 20% of the surface (Fig. 2). This model provides an excellent fit to both the shape and the absolute reflectance of 2005 FY9 at almost all near-infrared wavelengths with the exception of the region beyond 2.2 μm, where both the shape and absolute reflectance appear to require the presence of additional absorbers. At the low resolution of these spectra no positive identification of the absorber can be made.

Another location at which an additional absorber is required is in the visible part of the spectrum, blueward of about 0.7 μm, where methane has no strong absorption, yet the visible spectrum shows strong absorption. These red colorations, typical on many outer solar system objects, are traditionally assumed to be caused by tholins (Sagan & Khare 1979; Thompson et al. 1987)—complex mixtures of irradiated hydrocarbons—although direct evidence is difficult to obtain beyond the broadband visible colors and cosmochemical plausibility.

If we assume that the red visible color and the blue infrared color are both due to a single absorbing component, we derive an absorption spectrum reminiscent of the visible red, infrared blue tholins such as those created in gas-phase experiments intended to reproduce Titan hazes (Cruikshank et al. 1991). We cannot match the spectrum, however, by simply assuming that the nonmethane component is tholin, as having only 20% of the surface with a tholin-like spectrum cannot provide a sufficiently red optical spectrum. Some red component must be present within the methane component to match the optical spectrum.

3. HIGH-RESOLUTION SPECTROSCOPY

To continue our exploration of the composition and physical state of the surface of 2005 FY9 we obtained high-resolution ($R \sim 2500$) spectra on 2005 April 24 and 25 of selected near-infrared regions using NIRSPEC, the facility medium- to high-resolution spectrometer at the Keck telescope. The target was identified, centered into the 0.57″ slit, and tracked using the infrared slit-guiding camera. Observations consisted of series of 240 s integrations on two nod positions along the slit. For the *H*-band setting we obtained a total of 1.2 hr of on-source integration, and for the *K* band we obtained 3.4 hr of integration. All observations were performed at an air mass better than 1.2, and telluric calibration was performed by dividing by the spectrum of the nearby G5 star HD 109464, which was verified to have a solar-type spectrum by comparison to the more distant solar analog 47 UMa. Data reduction was performed as described in Brown (2000).

Figures 3 and 4 show the *H*- and *K*-band spectra of 2005 FY9 compared to the previously derived model of methane plus a featureless blue continuum. Like the lower resolution spectrum, the higher resolution spectrum closely matches the simple two-component model in most places. At a small number of locations,

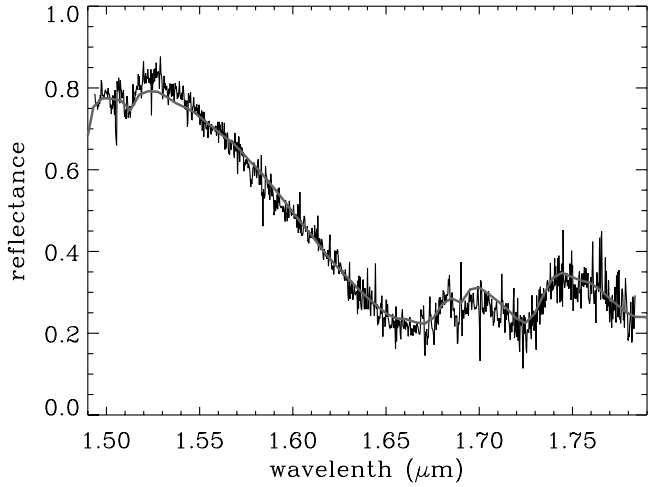

FIG. 3.—High-resolution spectrum of the *H*-band portion of the spectrum of 2005 FY9 (*black line*) compared to the simple low-resolution spectral model (*gray line*). The simple model provides an excellent fit even at higher resolution, although some mismatch occurs at regions of strong methane absorption between 1.68 and 1.77 μm. The spectral resolution in these higher resolution data is also approximately 2 pixels on the detector, so the point-to-point variation is again an accurate indicator of the size of the errors in the data.

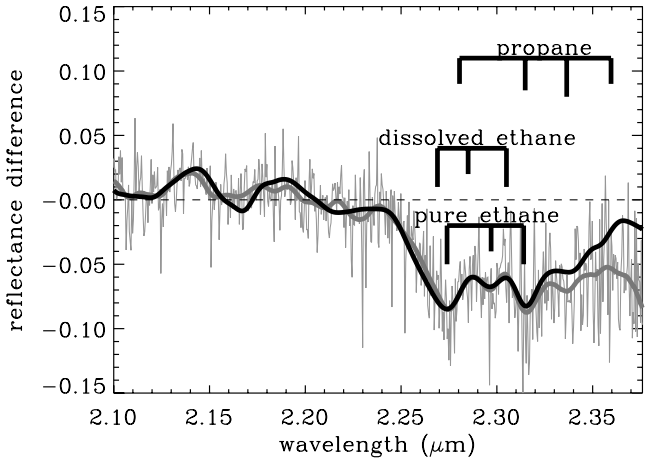

FIG. 5.—High-resolution *K*-band spectrum with the simple methane and blue continuum model subtracted (*thin gray line*). The thick gray line shows a smoothed view of the high-resolution spectrum. Of the simpler higher order hydrocarbons, only ethane and propane have features near the correct wavelengths. The straight solid lines indicate the wavelength and approximate strength of absorptions due to pure ethane, ethane dissolved in nitrogen, and propane. Of these, only ethane matches the three strongest absorptions. The spectrum beyond 2.25 μm is fitted with remarkable precision by the modeled spectrum of 100 μm ethane grains (*thick black line*). Even blueward of 2.25 μm many subtle features of the spectrum are explainable by the presence of ethane. The deviation of the model beyond 2.32 μm suggests the need for additional absorbers, of which propane appears a possible candidate.

most notably the previously identified region beyond 2.2 μm, additional potential absorption features appear. To determine the veracity of any potential additional absorption features we carefully examine each of the individual spectra to verify that the apparent absorption features are not caused by a single outlier in the data or a mismatch in the stellar and telluric calibration. In all cases these absorptions are robustly detected.

To further explore the spectra of the deviant regions we plot the difference between the simple methane–plus–blue component model spectrum and the higher resolution spectrum in Figure 5. Beyond 2.2 μm we see a series of blended absorption features. The saturation of the methane bands on 2005 FY9 leads to a much simpler spectrum in this region for methane and allows us to robustly measure this series of absorptions. Deep absorptions appear at 2.274 and 2.314 μm, with a weaker absorption at 2.296 μm between the two. General absorption with less distinct lines appears beyond 2.336 μm. Many hydrocarbon ices have features in these regions caused by the C-H stretch and its overtones, so the identification of features such as these is often difficult and inconclusive. Quirico et al. (1999) compared extensive laboratory measurements of many complex hydrocarbons in an attempt to match unidentified lines on Triton with no success. Examining their laboratory spectra (Quirico & Schmitt 1997), however, shows that one (and only one) of the many hydrocarbons that they measured in their laboratory has absorption features at the wavelengths of the three main absorption features above. Ethane has two strong absorptions at 2.274 and 2.314 μm and a weaker absorption at 2.297 μm between the two, just as our residual spectrum does. A model of 100 μm ethane grains constructed from the absorption coefficients of Quirico & Schmitt (1997) provides a precise match to the wavelength and absorption depths of the three main absorption features beyond 2.2 μm. In addition, the model even explains many of the features shortward of 2.2 μm that would otherwise be overlooked as unimportant. The only other hydrocarbon ice with absorption at some of the same wavelengths is propane. Ethane ice has additional overtone bands in the 1.6 μm range. A comparison of the difference spectrum in this region (Fig. 6) shows the same result: many of the features that would have been overlooked as simple mismatches of the methane spectrum are in fact fitted by the addition of the same amount of ethane that is required at the longer wavelengths. The match in wavelength of multiple lines and multiple bands along with the correct match in absorption depth for all of these features makes it clear that the identification of ethane on 2005 FY9 is conclusive.

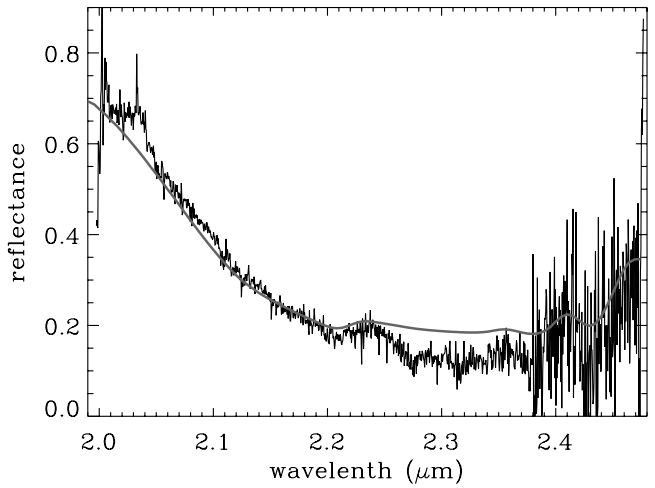

FIG. 4.—High-resolution spectrum of the *K*-band portion of the spectrum of 2005 FY9 (*black line*) compared to the simple low-resolution spectral model (*gray line*). The simple model provides an adequate fit at higher resolution, except from 2.00 to 2.05 μm, where the removal of telluric absorption is incomplete, and beyond 2.25 μm, where additional absorption is required.

Quirico & Schmitt (1997) also show that the dissolution of ethane in nitrogen causes a shift of the ethane lines to shorter wavelengths of 2.269, 2.285, and 2.305 μm. From the locations of these shifted lines, shown in Figure 5, it is clear that the ethane on 2005 FY9 is not dissolved in nitrogen.

While ethane provides an excellent fit to the residual spectrum, additional absorption is required between 1.54 and 1.61 μm, at 1.75 μm, and beyond 2.3 μm. The unexplained feature between

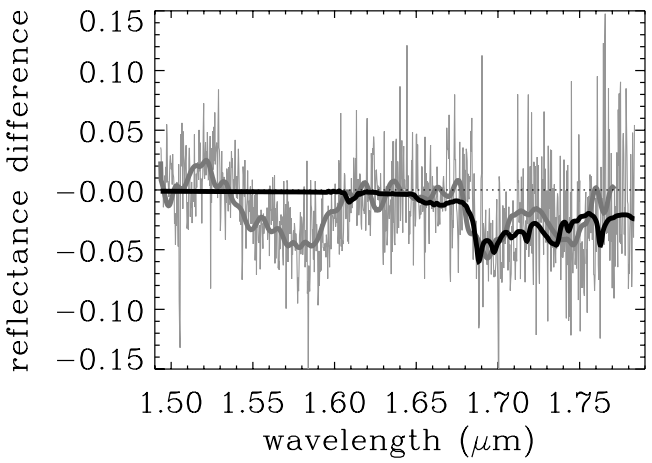

FIG. 6.—High-resolution *H*-band spectrum with the simple methane and blue continuum model subtracted (*thin gray line*). The thick gray line shows a smoothed view of the high-resolution spectrum. The black line shows the same ethane model used to fit the *K*-band spectrum. The general shape and location of the additional absorption beyond 1.68 μm matches that of the ethane model. An unexplained mismatch between the simple model and the high-resolution spectrum occurs between 1.54 and 1.61 μm. This feature could be due to an additional absorber, although its precise position and strength can be changed with slight changes in the simple methane model.

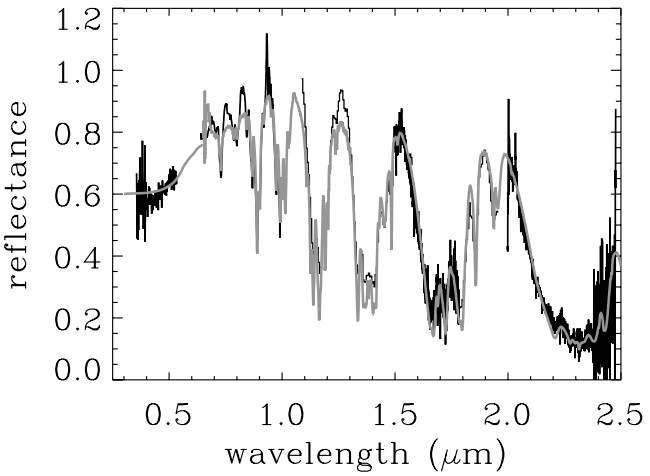

FIG. 7.—Complete spectral fit for 2005 FY9. The model uses 1 cm methane grains intimately mixed with 10 μm grains of tholin and 100 μm ethane grains in a 60 : 30 : 10 mix. All features of the spectrum are fitted, except for slight mismatches in the infrared continuum level. The continuum mismatches are well within the range of variation of the infrared reflectance of the many different possible tholin-type materials that might be present on the surface.

1.54 and 1.61 μm is on the shoulder of the methane absorption, and so its strength and precise position can be changed with slight changes in grain size in the simple methane model. No clear match to any known laboratory spectrum is apparent. The two additional absorptions also appear real, but no unique identification is possible. It seems likely, however, that if methane is being converted into ethane, then higher order hydrocarbons are also likely to be present. Propane is one of the next higher order hydrocarbons likely to be produced in this process, and the addition of propane to the spectrum provides a much better fit to the data beyond 2.30 μm. Nonetheless, we currently view this identification as inconclusive until better data beyond 2.30 μm are obtained.

We now attempt a complete spectral fit of the entire data set using all three of the identified components: methane, ethane, and a tholin. Unfortunately, a few different tholins have had optical constants measured, including those that appear to be the best match to the red optical, blue infrared component on 2005 FY9. We therefore artificially construct optical constants to match the bihemispheric reflectance spectrum of the gas-phase tholins shown in Cruikshank et al. (1991). While such artificially constructed optical constants are clearly insufficient for detailed modeling, they are used here to represent the general class of visible red, infrared blue tholins. A unique spectral model cannot be constrained by the data, so we instead attempt the simplest possible. We know that at least some part of the methane grains and the tholin grains must be intimately mixed, otherwise the red optical color could not be obtained, so we construct a model in which all three components are intimately mixed grains of different sizes. Figure 7 shows a model in which 1 cm methane grains, 100 μm ethane grains, and 10 μm tholin grains are intimately mixed in a 60:10:30 weight percentage ratio. All major features of the spectrum, including the red optical slope, the blue infrared continuum, the broad methane absorption lines from the visible to the infrared, and the ethane absorption in the infrared, are matched by this simple model.

Conspicuously absent in the spectrum is any hint of absorption by solid N_2 at 2.15 μm or by solid CO. On Pluto nitrogen is the dominant surface component, and much of the methane is dissolved inside the nitrogen. CO is also dissolved inside the nitrogen. Unfortunately, the absorption of N_2 at 2.15 μm is so weak that if methane is dissolved inside a nitrogen grain the methane has to be an almost insignificant component for the nitrogen line to even be visible. Using the absorption coefficients of Tryka et al. (1995) we find that we can represent the 1 cm grains of pure methane used in the above model equally well with nitrogen grains with only 5% methane dissolved within them. CO could likewise be present, but the absorption at 2.35 μm is in a region of thorough methane absorption saturation, so no feature could be seen. The CO feature at 1.577 μm, however, although weaker, is in a cleaner part of the spectrum. Modeling the CO spectrum using absorption coefficients from Quirico & Schmitt (1997) shows that this CO line would be detected if the CO abundance were as much as 20% that of the methane. While spectrally the main surface unit is dominated by methane, the actual surface unit could be as much as 95% nitrogen and 1% CO with only 4% methane, and it would appear identical. (Such a model would require correspondingly larger grain sizes to reach the required methane optical path lengths. If only 4% of the grain is methane, the grain must be 25 times larger, or approximately 25 cm.) While significant N_2 and CO could be hidden within the spectrum of 2005 FY9, it is clear that these ices are significantly depleted relative to their abundances of Pluto, where the nitrogen ice contains only about 0.5% methane and 0.1% CO dissolved within it (Douté et al. 1999).

4. DISCUSSION

The spectra of 2005 FY9 and that of Pluto appear similar in their dominance by absorption by methane, but in detail they are surprisingly distinct. The key features of the spectrum of 2005 FY9 include the large methane optical path lengths, the presence of ethane, the red visible and blue infrared continuum, and the lack of observable nitrogen or CO.

The large methane optical path lengths are perhaps the most surprising. Path lengths—parameterized as grain size but probably more physically thought of as distance between scattering defects in the ice—are a trade off between grain growth, which would eventually lead to arbitrarily large path lengths, and processes that break or remove the surface, including evaporation, cracking due to phase change, and surface bombardment. The small methane optical path lengths on Pluto are argued to be a

function of the small amount of methane dissolved in nitrogen ice and small grains of pure methane left when the more volatile nitrogen sublimes into the atmosphere and leaves a methane lag deposit.

The current heliocentric distance of 2005 FY9 of 52 AU and the visible albedo of 70% imply an equilibrium temperature of 29 K. At this temperature Clark et al. (1983) have estimated that the time required to grow grains to 1 cm would be $>10^{10}$ yr. Even at the perihelion distance of 38.7 and the equilibrium temperature of 34 K the grain growth time is $>10^{9}$ yr. The growth of these large optical path lengths on 2005 FY9 clearly cannot proceed through seasonal grain growth.

On Pluto and Triton similarly large path lengths are inferred for the majority nitrogen constituent. On these bodies nitrogen path lengths are thought to be long due to the fast sintering of small grains to form a polycrystalline slab from which voids are slowly removed over time (Eluszkiewicz 1991; Eluszkiewicz & Moncet 2003). On 2005 FY9, however, the large path lengths are found for methane rather than for nitrogen. In addition, no evidence for solid nitrogen is present. The large methane grains and the lack of observable nitrogen are perhaps related. If no or little nitrogen is present on 2005 FY9 and methane is instead the dominant surface component, the processes of polycrystalline growth and subsequent densification could operate on methane rather than nitrogen, and methane grains could grow on timescales longer than the orbital period. Methane on 2005 FY9 could grow to large polycrystalline slabs just as nitrogen on Pluto and Triton does.

Large methane grains, perhaps caused by a relative underabundance of nitrogen, also give a natural explanation for the much higher abundance of ethane on 2005 FY9 than on Pluto. Ethane is a natural product of UV irradiation of methane in both solid and gaseous form (Bar-Nun & Podolak 1979; Gupta et al. 1981; Khare et al. 1989; Hudson & Moore 1997; Krasnopolsky & Cruikshank 1999). On Pluto much of the methane is locked in a matrix of solid nitrogen, so when C-H bonds are broken in a methane molecule no adjacent methane molecule is present to combine to form longer chains, and the growth of complex hydrocarbons is stopped or slowed. The regions of pure methane on Pluto are thought to be thin, fine-grained lag deposits left behind as the nitrogen matrix evaporates. Small amounts of ethane could build up from photolysis of these layers, but these regions will be limited. Nakamura et al. (2000) suggest the detection of ethane on Pluto, although this claim is questioned by Cruikshank et al. (1999). The clear presence of ethane of 2005 FY9 bolsters the believability of this disputed feature on Pluto.

On 2005 FY9 methane is perhaps available in large relatively pure grains, giving abundant targets for UV photodestruction and then recombination into more complex hydrocarbons. Indeed, these large grains would be optically thick to the UV radiation responsible for the photolysis. These photons would be deposited within the upper few microns, so ethane and other higher order hydrocarbon formation would only occur at the upper layer of these grains, consistent with the small grain size for the ethane inferred.

This relationship between the methane grains and ethane formation leads us to our conceptual model of the surface of 2005 FY9. In our concept the surface is covered in polycrystalline methane with widely spaced voids and with a $\sim$100 μm rind of photolytically produced ethane on the upper surface of the methane. As this upper surface is the likely location of even higher order hydrocarbons, we also assume that it has mixed within it a component of tholin-like material.

All of the major differences between 2005 FY9 and Pluto appear explainable if methane rather than nitrogen is the dominant component on the surface of 2005 FY9, or perhaps if at least nitrogen is much less abundant on 2005 FY9 than on Pluto. The large methane path lengths appear natural for the dominant species, and the clear presence of ethane is a result of a higher density of methane available for photolytic reactions. However, depletion of nitrogen on 2005 FY9 is unexpected. Nitrogen is seen on Pluto and Triton, two larger bodies that also have methane. Nitrogen is even likely seen on Sedna, a similar-sized or smaller body. The reason for the apparent lack of this cosmochemically abundant volatile on 2005 FY9 is unknown.

While the hypothesis that nitrogen is underabundant on 2005 FY9 could be tested in principle by closely examining the wavelengths of methane lines to search for the shift due to dissolution in nitrogen, in practice the total saturation of many of the methane lines makes such a measurement of accurate line centers impossible. An occultation measurement of atmospheric pressure, however, would very quickly demonstrate the presence or absence of nitrogen, as a pure nitrogen surface would generate an atmosphere with a pressure 4 or 5 orders of magnitude greater than that of a pure methane atmosphere.

While 2005 FY9 appears to have a surface very different from that of Pluto, the surface of 2003 UB313 appears more closely related to that of Pluto. The methane spectrum on 2003 UB313 can be fitted with $\sim$100 μm grains, similar to those on Pluto. If our hypotheses for the cause of the difference between 2005 FY9 and Pluto is correct, we would then expect to find that 2003 UB313 is also dominated by nitrogen ice, leading to the small methane grains. Preliminary spectroscopy suggested that the methane was in a pure state (Brown et al. 2005), but better data should soon be available. With the discovery of 2005 FY9, 2003 UB313, and Sedna we now have a full class of methane-rich bodies in the outer solar system comparable to the previously unique Pluto and Triton. As with Pluto and Triton, detailed spectroscopic study will lead to insights into the surface and atmospheric processes of this new class of large outer solar system bodies.

This research is supported by the NASA planetary astronomy program through a Presidential Early Career award to M. E. B.

APPENDIX

SPECTRAL MODELS

The spectral modeling performed uses the bidirectional reflectance models of Hapke (1993). While in most cases excellent fits to the data can be obtained from these models, we view the physical description of the surface obtained from the best fits to be indicative of the general characteristics of the surface rather than prescriptive of the precise characteristics. In the spectral models we use characteristics of the spectral models to provide only gross insight into the surface, such as the ices present, the relative optical path lengths, and the broadband absorptions. For completeness, rather than for physical insight, we nonetheless describe the details of the models here.

Models of the geometric albedo as a function of wavelength are constructed using the diffuse reflectance approximation given in equation (10.38) of Hapke (1993). This approximation assumes that the surface is composed of a medium of anisotropic scatterers and that the spectrum includes contributions from initial single scattering and from multiple diffusive scattering. For our models we approximate the single-scattering particle albedo from an assumed particle size and a laboratory-derived absorption coefficient (using eq. [6.35] of Hapke), and we calculate the diffusive

reflectance from the single-scattering particle albedo (eqs. [8.22b] and [8.25] of Hapke). We then adjust the magnitude of the zero-phase single-scattering phase function to match the absolute albedo level (eq. [10.38] of Hapke). We do not explicitly model the opposition effect, as that effect is indistinguishable for the single-scattering phase function when only a single phase observation is available.

For the simple model of Figures 2–4 we model a surface that is 80% covered with 1 cm grains of methane and has an extremely high zero-phase phase function value of 3.0. The absorption coefficients of methane are obtained from Grundy et al. (2002). We linearly mix this spectrum with a nonphysical featureless blue continuum with 100% reflectance at 1 μm and 50% reflectance at 2.5 μm covering the remaining 20% of the surface. While we place little significance on the precise values of these parameters, the large grain sizes are a robust indicator of large optical path lengths, and the need for the blue component highlights the requirement for additional components on the surface.

The ethane models shown in Figures 5–6 are simple Hapke model of the reflectance of 100 μm isotropic grains of ethane, with the absorption coefficients taken from Quirico & Schmitt (1997).

The final spectral model, shown in Figure 7, is the simplest possible model that could provide a adequate match to the full spectrum. While more complex modeling is certainly possibly and likely even physically justified, we attempt only to show that this simple model can be used to match the data and provide gross properties. We construct the spectrum by using the mixing theory of Hapke (1993; eq. [10.61]) to construct bulk properties from an intimate mixture of ethane, methane, and tholin grains. The spectral mixture is constructed from a modeled surface with 70% by weight 1 cm methane grains, 20% 100 μm ethane grains, and the remainder an artificial approximation of the optical properties of a tholin. We construct the artificial approximation to the tholin component by estimating the single-scattering albedo of tholin from the bihemispheric reflectance spectrum of the gas-phase tholins shown in Cruikshank et al. (1991) by equations (8.25) and (10.23) of Hapke and assuming an arbitrary grain size. The derived optical properties are likely a poor representation of the true optical properties of this or any other tholin, but they spectrally represent the important visible red, infrared blue colors of the spectrum that are typical of many laboratory spectra of tholins.

REFERENCES

Barkume, K. M., Brown, M. E., & Schaller, E. L. 2005, BAAS, 37, 738
Bar-Nun, A., & Podolak, M. 1979, Icarus, 38, 115
Barucci, M. A., Cruikshank, D. P., Dotto, E., Merlin, F., Poulet, F., Dalle Ore, C., Fornasier, S., & de Bergh, C. 2005, A&A, 439, L1
Brown, M. E. 2000, AJ, 119, 977
Brown, M. E., Trujillo, C. A., & Rabinowitz, D. L. 2005, ApJ, 635, L97
Clark, R. N., Fanale, F. P., & Zent, A. P. 1983, Icarus, 56, 233
Cruikshank, D. P., Allamandola, L. J., Hartmann, W. K., Tholen, D. J., Brown, R. H., Matthews, C. N., & Bell, J. F. 1991, Icarus, 94, 345
Cruikshank, D. P., de Bergh, C., Doute, S., Geballe, T. R., Owen, T. C., Quirico, E., Roush, T. L., & Schmitt, B. 1999, Science, 285, 1355
Douté, S., Schmitt, B., Quirico, E., Owen, T. C., Cruikshank, D. P., de Bergh, C., Geballe, T. R., & Roush, T. L. 1999, Icarus, 142, 421
Eluszkiewicz, J. 1991, J. Geophys. Res., 96, 19217
Eluszkiewicz, J., & Moncet, J.-L. 2003, Icarus, 166, 375
Grundy, W. M., & Fink, U. 1996, Icarus, 124, 329
Grundy, W. M., Schmitt, B., & Quirico, E. 2002, Icarus, 155, 486
Gupta, S. K., Ochiai, E., & Ponnamperuma, C. 1981, Nature, 293, 725
Hapke, B. 1993, Theory of Reflectance and Emittance Spectroscopy (Cambridge: Cambridge Univ. Press)
Hudson, R. L., & Moore, M. H. 1997, Icarus, 126, 233
Khare, B. N., Thompson, W. R., Chyba, C. F., Sagan, C., & Arakawa, E. T. 1989, Adv. Space Res., 9, 41
Krasnopolsky, V. A., & Cruikshank, D. P. 1999, J. Geophys. Res., 104, 21979
Licandro, J., Pinilla-Alonso, N., Pedani, M., Oliva, E., Tozzi, G. P., & Grundy, W. M. 2006, A&A, 445, L35
Matthews, K., & Soifer, B. T. 1994, Exp. Astron., 3, 77
Nakamura, R., et al. 2000, PASJ, 52, 551
Oke, J. B., & Gunn, J. E. 1982, PASP, 94, 586
Quirico, E., Doute, S., Schmitt, B., de Bergh, C., Cruikshank, D. P., Owen, T. C., Geballe, T. R., & Roush, T. L. 1999, Icarus, 139, 159
Quirico, E., & Schmitt, B. 1997, Icarus, 127, 354
Rabinowitz, D. L., Schaefer, B. E., & Tourtellotte, S. W. 2007, AJ, in press
Rudy, R. J., Venturini, C. C., Lynch, D. K., Mazuk, S., Puetter, R. C., & Brad Perry, R. 2003, PASP, 115, 484
Sagan, C., & Khare, B. N. 1979, Nature, 277, 102
Thompson, W. R., Murray, B. G. J. P. T., Khare, B. N., & Sagan, C. 1987, J. Geophys. Res., 92, 14933
Trafton, L. M., & Stern, S. A. 1996, AJ, 112, 1212
Trujillo, C. A., & Brown, M. E. 2003, Earth Moon Planets, 92, 99
Tryka, K. A., Brown, R. H., & Anicich, V. 1995, Icarus, 116, 409